Measurement of the absolute branching ratio of the $K^+ \to \pi^+\pi^-\pi^+(\gamma)$ decay with the KLOE detector

KLOE/KLOE-2 Collaboration

D. Babusci [h], I. Balwierz-Pytko [g], G. Bencivenni [h], C. Bloise [h], F. Bossi [h], P. Branchini [r], A. Budano [q,r], L. Caldeira Balkeståhl [u], F. Ceradini [q,r], P. Ciambrone [h], F. Curciarello [i,d], E. Czerwiński [g], E. Danè [h], V. De Leo [i,d], E. De Lucia [h], G. De Robertis [b], A. De Santis [h], P. De Simone [h,*], A. Di Cicco [q,r], A. Di Domenico [m,n], R. Di Salvo [p], D. Domenici [h], O. Erriquez [a,b], G. Fanizzi [a,b], A. Fantini [o,p], G. Felici [h], S. Fiore [s,n], P. Franzini [m,n], A. Gajos [g], P. Gauzzi [m,n], G. Giardina [i,d], S. Giovannella [h], E. Graziani [r], F. Happacher [h], L. Heijkenskjöld [u], B. Höistad [u], T. Johansson [u], D. Kamińska [g], W. Krzemien [g], A. Kupsc [u], J. Lee-Franzini [h,t], F. Loddo [b], S. Loffredo [q,r], G. Mandaglio [i,d,c], M. Martemianov [j], M. Martini [h,l], M. Mascolo [o,p], R. Messi [o,p], S. Miscetti [h], G. Morello [h], D. Moricciani [p], P. Moskal [g], A. Palladino [h], A. Passeri [r], V. Patera [k,h], I. Prado Longhi [q,r], A. Ranieri [b], P. Santangelo [h], I. Sarra [h], M. Schioppa [e,f], B. Sciascia [h], M. Silarski [g], L. Tortora [r], G. Venanzoni [h], W. Wiślicki [v], M. Wolke [u]

[a] Dipartimento di Fisica dell'Università di Bari, Bari, Italy
[b] INFN Sezione di Bari, Bari, Italy
[c] Centro Siciliano di Fisica Nucleare e Struttura della Materia, Catania, Italy
[d] INFN Sezione di Catania, Catania, Italy
[e] Dipartimento di Fisica dell'Università della Calabria, Cosenza, Italy
[f] INFN Gruppo collegato di Cosenza, Cosenza, Italy
[g] Institute of Physics, Jagiellonian University, Cracow, Poland
[h] Laboratori Nazionali di Frascati dell'INFN, Frascati, Italy
[i] Dipartimento di Fisica e Scienze della Terra dell'Università di Messina, Messina, Italy
[j] Institute for Theoretical and Experimental Physics (ITEP), Moscow, Russia
[k] Dipartimento di Scienze di Base ed Applicate per l'Ingegneria dell'Università "Sapienza", Roma, Italy
[l] Dipartimento di Scienze e Tecnologie applicate, Università "Guglielmo Marconi", Roma, Italy
[m] Dipartimento di Fisica dell'Università "Sapienza", Roma, Italy
[n] INFN Sezione di Roma, Roma, Italy
[o] Dipartimento di Fisica dell'Università "Tor Vergata", Roma, Italy
[p] INFN Sezione di Roma Tor Vergata, Roma, Italy
[q] Dipartimento di Matematica e Fisica dell'Università "Roma Tre", Roma, Italy
[r] INFN Sezione di Roma Tre, Roma, Italy
[s] ENEA UTTMAT-IRR, Casaccia R.C., Roma, Italy
[t] Physics Department, State University of New York at Stony Brook, USA
[u] Department of Physics and Astronomy, Uppsala University, Uppsala, Sweden
[v] National Centre for Nuclear Research, Warsaw, Poland

ARTICLE INFO

ABSTRACT

The absolute branching ratio of the $K^+ \to \pi^+\pi^-\pi^+(\gamma)$ decay, inclusive of final-state radiation, has been measured using ~ 17 million tagged K^+ mesons collected with the KLOE detector at DAΦNE, the Frascati ϕ-factory. The result is:

$$\mathrm{BR}(K^+ \to \pi^+\pi^-\pi^+(\gamma)) = 0.05565 \pm 0.00031_{stat} \pm 0.00025_{syst}$$

* Corresponding author.
 E-mail address: patrizia.desimone@lnf.infn.it (P. De Simone).

a factor $\simeq 5$ more precise with respect to the previous result. This work completes the program of precision measurements of the dominant kaon branching ratios at KLOE.

1. Introduction

The measurement of the branching ratio (BR) of $K^+ \to \pi^+\pi^-\pi^+(\gamma)$ decay completes the KLOE program of precision measurements of the dominant kaon branching ratios, fully inclusive of radiation effects. We have already published an evaluation, from a fit to the KLOE measurements of the charged kaon lifetime [1], and BRs, [2–5], constraining the BR sum to unity: BR$(K^\pm \to \pi^\pm\pi^+\pi^-) = (5.68 \pm 0.22)\%$ [5]. The most recent BR$(K^\pm \to \pi^\pm\pi^+\pi^-)$ measurement, based on 2330 events from a sample of $\sim 10^5$ kaon decays, dates back to 1972 and gives no information on the radiation cut-off: BR$(K^\pm \to \pi^\pm\pi^+\pi^-) = (5.56 \pm 0.20)\%$ [6]. The PDG value, BR$(K^\pm \to \pi^\pm\pi^+\pi^-) = (5.59 \pm 0.04)\%$ [7], is obtained from a global fit that does not use any of the available BR$(K^\pm \to \pi^\pm\pi^+\pi^-)$ measurements but the rate measurement $\Gamma(\pi^+\pi^+\pi^-) = (4.511 \pm 0.024) \times 10^6$ s^{-1} published in 1970 [8]. Furthermore the BR$(K^\pm \to \pi^\pm\pi^+\pi^-)$ value enters in the evaluation of the difference $a_0 - a_2$ between the $I = 0$ and $I = 2$ S-wave $\pi\pi$ scattering lengths [16,19]; this will be discussed in Section 5.

In the following we report the measurement of the absolute branching ratio BR$(K^+ \to \pi^+\pi^-\pi^+(\gamma))$ performed with the KLOE detector using data corresponding to an integrated luminosity $\int \mathcal{L}\,dt \simeq 174$ pb^{-1} collected at DAΦNE, the Frascati ϕ-factory [9]. DAΦNE is an e^+e^- collider operated at the energy of 1020 MeV, the mass of the ϕ-meson. The beams collide at the interaction point (IP) with a crossing angle $\theta_x \simeq 25$ mrad,[1] producing ϕ-mesons with a small momentum of ~ 12.5 MeV in the horizontal plane. The ϕ-mesons decay in anti-collinear and monochromatic neutral (34%) and charged (49%) kaon pairs. The unique feature of a ϕ-factory is the tagging: detection of a $K^\pm$ (the tagging kaon) tags the presence of a $K^\mp$ (the tagged kaon) with known momentum and direction. The availability of tagged kaons enables the precision measurement of absolute BRs providing the normalization sample. The decay products of the K^+K^- pair define two spatially well separated regions called in the following the tag and the signal hemispheres.

2. The KLOE detector

The KLOE detector consists of a large cylindrical drift chamber (DC) [10], surrounded by a lead scintillating fiber electromagnetic calorimeter (EMC) [11] both immersed in an axial 0.52 T magnetic field produced by a superconducting coil. At the beams IP the spherical beam pipe of 10 cm radius is made of a beryllium–aluminum alloy of 0.5 mm thickness.

The DC tracking system has 25 cm internal radius, 4 m diameter and 3.3 m length, with a total of $\sim 52\,000$ wires, of which $\sim 12\,000$ are sense wires arranged in a stereo geometry. In order to minimize the multiple scattering and K_L regeneration, and to maximize the detection efficiency for low energy photons, the DC works with a helium-based gas mixture and its walls are made of light materials, mostly carbon fiber composites. Spatial resolutions

are $\sigma_{xy} \simeq 150$ μm and $\sigma_z \simeq 2$ mm and the transverse momentum resolution is $\sigma(p^T)/p^T \leq 0.4\%$.

The calorimeter covers 98% of the solid angle and is composed by a barrel and two endcaps. Particles showering in the lead-scintillator-fiber EMC structure are detected as local energy deposits by clustering signals from read-out elements. For each impinging particle the calorimeter information consists of energy, position of impact point and time of arrival with accuracies of $\sigma_E/E = 5.7\%/\sqrt{E \text{ (GeV)}}$, $\sigma_z = 1.2$ cm$/\sqrt{E \text{ (GeV)}}$, $\sigma_\phi = 1.2$ cm, and $\sigma_t = 57$ ps$/\sqrt{E \text{ (GeV)}} \oplus 100$ ps. Energy clusters not associated with reconstructed tracks in the DC (neutral clusters) identify neutral particles. The definition of energy clusters associated with reconstructed tracks is related to the track-to-cluster association procedure described in Ref. [12].

The trigger [13] is based on energy deposits in the calorimeter and on hit multiplicity in the drift chamber. Only events triggered by the calorimeter have been used in the present analysis. The trigger system includes a second-level veto for cosmic-ray muons (cosmic-ray veto or CRV) based on energy deposits in the outermost layers of the calorimeter and followed by a third-level software trigger. A software filter (SF), based on the topology and multiplicity of energy clusters and drift chamber hits, is applied to filter out machine background. Both CRV and SF may be sources of events loss. Their effect on the BR measurement has been studied on control data samples acquired respectively without the CRV and the SF filters.

The data sample used for this analysis has been processed and filtered with the KLOE standard reconstruction software and the event classification procedure [12]. The KLOE Monte Carlo (MC) simulation package, GEANFI, has been used to produce a sample equivalent to data, accounting for the detector status and the machine operation on a run-by-run basis.

3. Analysis strategy

Tagging with K$^\pm \to \mu^\pm\nu(\gamma)$ ($K_{\mu 2}$ tags) and K$^\pm \to \pi^\pm\pi^0(\gamma)$ ($K_{\pi 2}$ tags) provides two indipendent samples of pure kaons for the signal selection useful for systematic uncertainties evaluation and cross-checks [3]. These decays are easily identified as clear peaks in the distribution of p$^*_{m_\pi}$, the momentum of the charged secondary track in the kaon rest frame evaluated using the pion mass.[2] The selection efficiency of the two tagging normalization samples are similar, about 36%. Then these events are classified as $\phi \to K^+K^-$ and archived in dedicated data summary tapes, as described in Ref. [12]. MC studies show that the contamination due to ϕ-meson decays other than K^+K^- is negligible.

To minimize the impact of the trigger efficiency on the signal side, we choose as normalization sample $K_{\mu 2}$ or $K_{\pi 2}$ tags providing the trigger of the event (self-triggering two-body decays). After this request the $K_{\mu 2}$ sample is reduced by a factor of $\sim 33\%$, while the $K_{\pi 2}$ sample by a factor of $\sim 43\%$. The residual dependence of the signal sample on the tag selection, which we refer

---

[1] We use left-handed coordinates system with the z-axis defined as the bisectrix of the e^+e^- beams and the y-axis vertical.

[2] The contribution to the p$^*_{m_\pi}$ distribution from $K_{\mu 2}$ decays is slightly broadened due to the pion mass hypothesis [3].

to as tag bias, has been evaluated for the BR measurement. Moreover we use K^- as the tagging kaon ($K_{\mu2}$ or $K_{\pi2}$) and K^+ as the tagged kaon (signal), since the nuclear cross section for positive kaons with momenta $\simeq 100$ MeV is lower by a factor of $\sim 10^3$ with respect to that of negative kaons [14].

The track of the tagging kaon is backward extrapolated from its first hit in the DC to the IP. We use the momentum of the tagging kaon at the IP, $\mathbf{p}_{K^-}^{IP}$, and the momentum of the ϕ-meson measured run by run with Bhabha scattering events, $\mathbf{p}_\phi$, to evaluate the momentum of the tagged kaon at the IP, $\mathbf{p}_{K^+}^{IP} = \mathbf{p}_\phi - \mathbf{p}_{K^-}^{IP}$. Finally we extrapolate $\mathbf{p}_{K^+}^{IP}$ inside the DC (signal kaon path).

The kaon and the three charged pions from its decay have low momenta, less than ~ 200 MeV, and curl up in the KLOE magnetic field; this increases the probability to have poorly reconstructed tracks broken in more segments (the track reconstruction procedure in KLOE is described in Ref. [12]). We significantly improve the quality of the reconstruction requiring the K^+ decay to occur before it reaches the DC sensitive volume, i.e. inside a cylindrical fiducial volume centered at the IP and with a transverse radius ρ_{xy} close to the DC inner wall (detector acceptance $\sim 26\%$). In this way only the pion tracks are reconstructed, and we extrapolate only two of them to search for a vertex along the signal kaon path. No further request on the charge of the particles is applied to maximize the selection efficiency.

To extract the number of $K^+ \to \pi^+\pi^-\pi^+(\gamma)$ we fit the missing mass spectrum $m_{miss}^2 = E_{miss}^2 - (\mathbf{p}_{K^+} - \mathbf{p}_1 - \mathbf{p}_2)^2$ where $\mathbf{p}_1$ and $\mathbf{p}_2$ are the momenta of the selected tracks, with MC-predicted shapes for the signal and the background. The branching ratio is given by:

$$\text{BR}\big(K^+ \to \pi^+\pi^-\pi^+(\gamma)\big) = \frac{N_{K\to3\pi}}{N_{tag}} \times \frac{1}{\epsilon_{sel}C_{TB}C_{SF}C_{CRV}} \qquad (1)$$

where $N_{K\to3\pi}$ is the number of signal events, N_{tag} is the number of tagged events and ϵ_{sel} is the overall signal selection efficiency, including the detector acceptance and the reconstruction efficiency. C_{SF} and C_{CRV} are the corrections for the machine background filter and the cosmic-ray veto. C_{TB} accounts for the tag bias effect.

3.1. BR measurement with the $K_{\mu2}^-$ normalization sample

The normalization sample is given by $N_{tag} = 12\,065\,087$ $K_{\mu2}^-$ tagging events. The $K^+ \to \pi^+\pi^-\pi^+(\gamma)$ signal selection uses DC information only.

Any reconstructed track identified as a K^+ (and therefore corresponding to a K^+ outside the fiducial volume) is rejected. More specifically we reject tracks with the point of closest approach (PCA) to the IP satisfying the conditions $\sqrt{x_{PCA}^2 + y_{PCA}^2} < 10$ cm, and $|z_{PCA}| < 20$ cm, with the momentum within $70 < p_K < 130$ MeV, and with a good matching with the position and the momentum extrapolated from the tagging kaon.

To select the decay vertex $K^+ \to \pi^+\pi^-\pi^+(\gamma)$ we require at least two reconstructed tracks that have:

(1) momentum in the kaon rest frame, $p_{m_\pi}^* < 190$ MeV, this cut removes the background from two-body decays;
(2) distance of closest approach (DCA) between each extrapolated track and the signal kaon path, DCA < 3 cm;
(3) distance of closest approach between the two tracks, DCA$_{12} < 3$ cm;
(4) the opening angle between the momenta of the two tracks, $|\cos(\theta_{12})| < 0.9$, this cut removes the background due to residual kaon broken tracks;
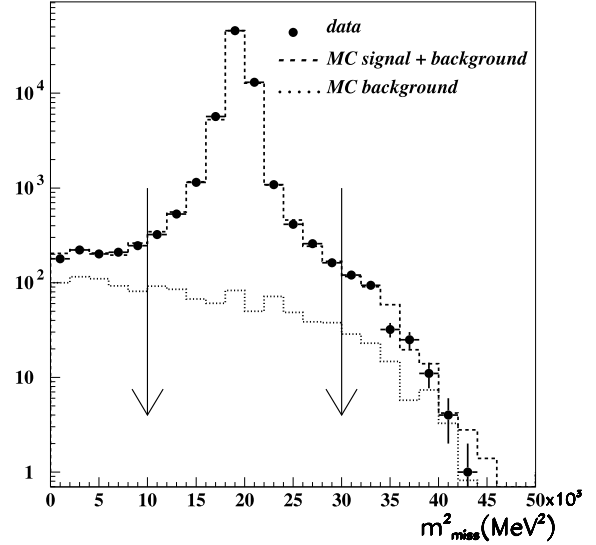(5) the decay vertex is accepted in the fiducial volume, $\rho_{xy} \leq 26$ cm.

Fig. 1. MC (dashed) and data (points) missing mass spectrum of the selected events. The arrows show the missing mass window for signal counting.
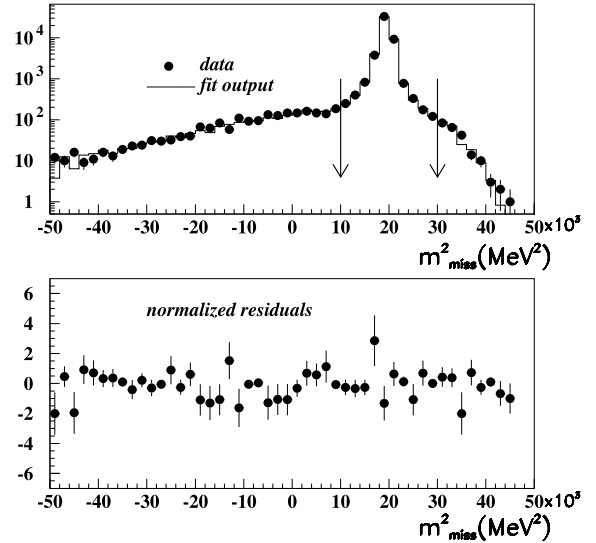

Fig. 2. Top plot: fit of the missing mass spectrum superimposed with data points. Bottom plot: residuals between the output of the fit and data distribution normalized to their errors.

Fig. 1 shows the comparison between MC and data missing mass distributions for the selected K^+ decays. We count the number of signal events in the missing mass window $10\,000 < m_{miss}^2 < 30\,000$ MeV^2, where the signal over background ratio is $S/B \simeq 88$. The background composition is given by K^+ in two-body $\mu^+\nu$ and $\pi^+\pi^0 \simeq 0.1\%$, semileptonic $\pi^0 e^+\nu$ and $\pi^0\mu^+\nu \simeq 0.5\%$, and $\pi^+\pi^0\pi^0 \simeq 0.4\%$ decays. These single track events pass the selection criteria because a secondary charged track is wrongly reconstructed as two separate tracks. The top panel of Fig. 2 shows the result of the fit of the missing mass distribution compared to data. The fit gives $N_{K\to3\pi} = 48\,032 \pm 286$ signal events (the error accounting for data and MC statistics), with $\chi^2/\text{ndf} = 44.8/46$ ($P(\chi^2) = 0.52$). The bottom panel of Fig. 2 shows the fit normalized residuals.

The signal selection efficiency, ϵ_{sel}, is related to the track reconstruction efficiency of two charged secondaries from K^+ decays. We evaluate the selection efficiency from MC, and then we correct it to take into account data-MC differences in the track

Table 1

Corrections to BR($K^+ \to \pi^+\pi^+\pi^-(\gamma)$) measurement. The events selected by the two tags have different topologies in the KLOE detector determining different corrections factors.

Table of corrections	$K^-_{\mu 2}$ tags	$K^-_{\pi 2}$ tags
cosmic ray veto correction C_{CRV}	1.00125 ± 0.00002	1.00049 ± 0.00001
software filter correction C_{SF}	1.0144 ± 0.0013	1.0003 ± 0.0005
tag bias correction C_{TB}	0.839 ± 0.001	0.802 ± 0.002

Table 2

Summary table of the fractional statistical uncertainties.

Source of statistical uncertainties	$K^-_{\mu 2}$ tags (%)	$K^-_{\pi 2}$ tags (%)
signal counting	0.45	0.70
selection efficiency	0.38	0.60
tag bias	0.11	0.18
software filter	0.13	0.05
cosmic ray veto	0.002	0.0005
Total fractional statistical uncertainty	0.62	0.95

reconstruction. To this aim we select, both on data and MC, a control sample of $K^+ \to \pi^- X$ decays (for signal events X corresponds to $\pi^+\pi^+$). The first requirement is the presence of a self-triggering $K^-_{\mu 2}$ in the tag hemisphere. Then the track of the π^- candidate is selected with the following requirements:

(1) the number of neutral clusters with an energy $E_\gamma \geq 30$ MeV must be, $N_{clusters} \leq 1$;
(2) the momentum of the selected track in the kaon rest frame must be, $p^*_{m_\pi} \leq 130$ MeV;
(3) the distance of closest approach between the extrapolated track and the signal kaon path must be, DCA$_{\pi -} < 7$ cm;
(4) the cosine of the opening angle between the momenta of the signal kaon and the momenta of the selected track must be, $\cos(\theta_{K\pi}) \leq -0.85$.

The control sample $K^+ \to \pi^- X$, selected with a background contamination of $\simeq 10.7\%$, is used to measure the efficiency corrections as function of the total transverse momentum p^T_X, and of the total longitudinal momentum p^L_X of the $\pi^+\pi^+$ pair (the average efficiency correction is ~ 0.92). The selection efficiency, is finally obtained folding the MC selection efficiency with the measured corrections: $\epsilon_{sel} = 0.0842 \pm 0.0003$.

The corrections C_{CRV} and C_{SF} have been measured with data taken without the cosmic-ray veto and the software filter, respectively. The correction for the tag bias, C_{TB}, has been evaluated using MC. All correction values are reported in Table 1.

The summary of the fractional statistical uncertainties is reported in Table 2. The total statistical fractional uncertainty on the branching ratio measurement is 0.62%.

3.2. BR measurement with the $K^-_{\pi 2}$ normalization sample

The normalization sample is given by $N_{tag} = 5\,171\,239$ $K^-_{\pi 2}$ tagging events.

The signal selection described in Subsection 3.1 is also applied to the sample tagged by $K^-_{\pi 2}$ decays. The fit to the missing mass spectrum of the selected events gives $N_{K \to 3\pi} = 20\,063 \pm 186$ signal events with $\chi^2/\text{ndf} = 42.9/45$ (P(χ^2) = 0.56). The signal over background ratio in the missing mass window $10\,000 < m^2_{miss} < 30\,000$ MeV^2 is evaluated with MC: $S/B \simeq 84$.

To evaluate the selection efficiency, we used the corrections measured with the control sample $K^+ \to \pi^- X$ tagged by $K^-_{\mu 2}$ events. The selection efficiency for signal events tagged by $K^-_{\pi 2}$ events, is: $\epsilon_{sel} = 0.0866 \pm 0.0005$.

Table 3

Summary table of the fractional systematic uncertainties.

Source of systematic uncertainties	$K^-_{\mu 2}$ tags (%)	$K^-_{\pi 2}$ tags (%)
DCA, DCA$_{12}$, $\cos(\theta_{12})$ cuts	0.52	0.41
p$^*_{m_\pi}$ cut	0.08	0.11
m^2_{miss} cut	0.05	0.14
fiducial volume	0.11	0.10
selection efficiency estimate	0.16	0.16
tag bias	0.16	0.32
$K^\pm$ lifetime	0.12	0.12
Total fractional systematic uncertainty	0.60	0.59

The summary of the fractional statistical uncertainties is reported in Table 2. The total statistical fractional uncertainty on the branching ratio measurement using the $K^-_{\pi 2}$ tagging sample is 0.95%.

4. Systematic uncertainties

The following sources of systematic uncertainties on the branching ratios measured using both tags, $K^-_{\mu 2}$ and $K^-_{\pi 2}$, have been considered:

(1) the cuts used to select the signal sample;
(2) the fiducial volume;
(3) the cuts used to select the control sample $K^+ \to \pi^- X$;
(4) the cuts used to select the tagging samples $K^-_{\mu 2}$ and $K^-_{\pi 2}$;
(5) the charged kaon lifetime.

The corresponding systematic uncertainties are listed in Table 3.

The contributions to the systematic error due to points (1), (2), and (3) have been evaluated varying the selection cuts. The DCA, DCA$_{12}$ variables and the fiducial volume ρ_{xy} have been varied within few sigmas, the cuts on $\cos(\theta_{12})$, $p^*_{m_\pi}$ and m^2_{miss} have been varied to decrease the S/B ratio to $\simeq 64$. The cuts used to select the control sample $K^+ \to \pi^- X$ have been varied to increase the background contamination up to $\simeq 20\%$.

Concerning the selection of the normalization samples (point (4)) we have evaluated the effect of a C_{TB} variation on the BR measurements. This has been done modifying the selection of the data and MC normalization samples adding a cut on the opening angle between the K^- track and the secondary track retaining events with $\cos(\theta_{Kt}) \geq 0$, where t is the μ^- (π^-) track in case of the $K^-_{\mu 2}$ ($K^-_{\pi 2}$) sample. Using MC we found that the fractional variations of the tag bias corrections are $\delta C_{TB}/C_{TB}(K^-_{\mu 2}) = 0.26\%$ and $\delta C_{TB}/C_{TB}(K^-_{\pi 2}) = 0.63\%$. Consequently the branching ratios measured values change of $\delta\,\text{BR}/\text{BR}(K^-_{\mu 2}) = 0.32\%$ and $\delta\,\text{BR}/\text{BR}(K^-_{\pi 2}) = 0.64\%$; half of these variations have been assigned as conservative values for the fractional systematic uncertainties due to the tag bias (see Table 3).

The BR($K^+ \to \pi^+\pi^+\pi^-(\gamma)$) depends on the charged kaon lifetime $\tau_{K\pm}$ through the detector acceptance, that is evaluated with MC simulation (point (5)). The systematic effect has been obtained varying $\tau_{K\pm}$ within the uncertainty of the KLOE result $\tau_{K\pm} = 12.347 \pm 0.030$ ns [1]. This has been done re-weighting the MC events with a hit-or-miss procedure, both for the signal and the control sample selection procedures. The corresponding systematic errors are listed in Table 3.

The analysis is fully inclusive of radiative decays. Only the efficiency evaluation could be affected by a systematic uncertainty due to the cut $N_{clusters} \leq 1$ (see Subsection 3.1). We have used PHOTOS [15] to evaluate such an effect and we obtained a negligible contribution, being $O(10^{-6})$ the fraction of decays removed by the cut $N_{clusters} \leq 1$.

Table 4
Results of the fit: $K^{\pm}$ BRs and correlation coefficients.

Parameter	Value	Correlation coefficients					
$\mathrm{BR}(K_{\mu 2}^{\pm})$	0.6372(11)						
$\mathrm{BR}(K_{\pi 2}^{\pm})$	0.2070(9)	0.55					
$\mathrm{BR}(\pi^{\pm}\pi^{-}\pi^{+})$	0.0558(4)	−0.23	−0.05				
$\mathrm{BR}(K_{e3}^{\pm})$	0.0498(5)	0.42	−0.15	0.06			
$\mathrm{BR}(K_{\mu 3}^{\pm})$	0.0324(4)	−0.39	0.14	−0.05	−0.58		
$\mathrm{BR}(\pi^{\pm}\pi^{0}\pi^{0})$	0.01764(25)	−0.13	0.05	−0.02	0.04	−0.04	
$\tau_{K^{\pm}}$ (ns)	12.344(29)	0.20	0.19	−0.14	0.05	−0.04	0.02

The fraction of K^{+} undergoing nuclear interactions is negligible, $\sim 10^{-5}$, as evaluated using the MC simulation, based on data available in literature [14]. Therefore the related systematic uncertainty is negligible.

Furthermore we have checked on two independent sub-samples of about 88 pb^{-1} and 86 pb^{-1} that the efficiency corrections and the BR evaluations are not correlated.

Finally the stability of the measurements with respect to different data taking periods and conditions has been checked.

5. Results

With a sample of $K^{-} \rightarrow \mu^{-}\bar{\nu}(\gamma)$ tagging events $N_{tag} = 12\,065\,087$ we found $N_{K \rightarrow 3\pi} = 48\,032 \pm 286$ signal events. Using Eq. (1), we obtain the branching ratio:

$$\mathrm{BR}\left(K^{+} \rightarrow \pi^{+}\pi^{-}\pi^{+}(\gamma)\right)\big|_{Tag\,K_{\mu 2}}$$
$$= 0.05552 \pm 0.00034_{stat} \pm 0.00034_{syst}. \qquad (2)$$

With a sample of $K^{-} \rightarrow \pi^{-}\pi^{0}(\gamma)$ tagging events $N_{tag} = 5\,171\,239$ we found $N_{K \rightarrow 3\pi} = 20\,063 \pm 186$ signal events, corresponding to:

$$\mathrm{BR}\left(K^{+} \rightarrow \pi^{+}\pi^{-}\pi^{+}(\gamma)\right)\big|_{Tag\,K_{\pi 2}}$$
$$= 0.05587 \pm 0.00053_{stat} \pm 0.00033_{syst}. \qquad (3)$$

Averaging these two results, accounting for correlations, we obtain:

$$\mathrm{BR}\left(K^{+} \rightarrow \pi^{+}\pi^{-}\pi^{+}(\gamma)\right) = 0.05565 \pm 0.00031_{stat} \pm 0.00025_{syst}.$$
$$(4)$$

This absolute branching ratio measurement is fully inclusive of final-state radiation and has a 0.72% accuracy, a factor $\simeq 5$ better with respect to the previous measurement [6].

We fit the six largest $K^{\pm}$ BRs and the lifetime $\tau_{K}^{\pm}$ using the KLOE measurements of $\tau_{K^{\pm}}$ [1], $\mathrm{BR}(K_{\mu 2}^{+})$ [2], $\mathrm{BR}(K_{\pi 2}^{+})$ [5], $\mathrm{BR}(K^{+} \rightarrow \pi^{+}\pi^{-}\pi^{+}(\gamma))$ (Eq. (4)), $\mathrm{BR}(K_{l3}^{\pm})$ [3], and $\mathrm{BR}(K^{\pm} \rightarrow \pi^{\pm}\pi^{0}\pi^{0})$ [4], with their dependence on $\tau_{K}^{\pm}$, and imposing the constraint $\sum \mathrm{BR}(K^{\pm} \rightarrow f) = 1$. The fit results, with $\chi^{2}/\mathrm{ndf} = 0.24/1$ (CL = 0.63), show a coherent set of measurements (see Table 4).

The NA48 experiment observed in the $\pi^{0}\pi^{0}$ invariant mass distribution a cusp-like anomaly at $M_{00} = 2m_{\pi^{+}}$ [16], which has been interpreted as mainly due to the final state charge–exchange reaction $\pi^{+}\pi^{-} \rightarrow \pi^{0}\pi^{0}$ in $K^{\pm} \rightarrow \pi^{\pm}\pi^{+}\pi^{-}$ decay [17,18]. The fit to the M_{00}^{2} distribution [19] with two different models [20] and [21, 22] determines $a_{0} - a_{2}$, the difference between the S-wave $\pi\pi$ scattering lengths in the isospin $I = 0$ and $I = 2$ states. In this calculation the main source of uncertainty is the ratio of the weak amplitudes of $K^{\pm} \rightarrow \pi^{\pm}\pi^{-}\pi^{+}$ and $K^{\pm} \rightarrow \pi^{\pm}\pi^{0}\pi^{0}$ decay, that is obtained from the ratio R of the branching ratio values. Using the $\mathrm{BR}(\pi^{\pm}\pi^{-}\pi^{+})$, $\mathrm{BR}(\pi^{\pm}\pi^{0}\pi^{0})$ and their correlation shown in Table 4 we evaluate $R = 3.161 \pm 0.049$, in agreement with the value

$R = 3.175 \pm 0.050$ obtained by NA48 [19] with BRs from the PDG fit [7].

6. Conclusions

We have measured the absolute branching ratio of the $K^{+} \rightarrow \pi^{+}\pi^{-}\pi^{+}(\gamma)$ decay, inclusive of final-state radiation, using two indipendent normalization samples from $K_{\mu 2}^{-}$ and $K_{\pi 2}^{-}$ tags:

$$\mathrm{BR}\left(K^{+} \rightarrow \pi^{+}\pi^{-}\pi^{+}(\gamma)\right) = 0.05565 \pm 0.00031_{stat} \pm 0.00025_{syst}$$

with an overall accuracy of 0.72%. This measurement completes the KLOE program of precision measurements of the dominant kaon branching ratios.

References

[1] KLOE Collaboration, F. Ambrosino, et al., J. High Energy Phys. 01 (2008) 73.
[2] KLOE Collaboration, F. Ambrosino, et al., Phys. Lett. B 632 (2006) 76.
[3] KLOE Collaboration, F. Ambrosino, et al., J. High Energy Phys. 02 (2008) 98.
[4] KLOE Collaboration, A. Aloisio, et al., Phys. Lett. B 597 (2004) 139.
[5] KLOE Collaboration, F. Ambrosino, et al., Phys. Lett. B 666 (2008) 15.
[6] I.H. Chiang, et al., Phys. Rev. D 6 (1972) 1254.
[7] PDG, Phys. Rev. D 86 (2012) 010001.
[8] W.T. Ford, et al., Phys. Rev. Lett. 25 (1970) 1370.
[9] A. Drago, et al., LNF-03/012, 2003.
[10] KLOE Collaboration, M. Adinolfi, et al., Nucl. Instrum. Methods 488 (2002) 51.
[11] KLOE Collaboration, M. Adinolfi, et al., Nucl. Instrum. Methods 482 (2002) 364.
[12] KLOE Collaboration, F. Ambrosino, et al., Nucl. Instrum. Methods 534 (2004) 403.
[13] KLOE Collaboration, M. Adinolfi, et al., Nucl. Instrum. Methods 492 (2002) 134.
[14] C.B. Dover, G.E. Walker, The interaction of kaons with nucleons and nuclei, Phys. Rep. 89 (1982) 1–177.
[15] E. Barberio, B. van Eijk, Z. Was, Comput. Phys. Commun. 66 (1991) 115.

[16] NA48 Collaboration, J.R. Batley, et al., Phys. Lett. B 633 (2006) 173.
[17] P. Budini, L. Fonda, Phys. Rev. Lett. 6 (1961) 419.
[18] N. Cabibbo, Phys. Rev. Lett. 93 (2004) 121801.
[19] NA48 Collaboration, J.R. Batley, et al., Eur. Phys. J. B 64 (2009) 589.

[20] N. Cabibbo, G. Isidori, J. High Energy Phys. 0503 (2005) 21.
[21] G. Colangelo, J. Gasser, B. Kubis, A. Rusetsky, Phys. Lett. B 638 (2006) 187.
[22] M. Bissegger, A. Fuhrer, J. Gasser, B. Kubis, A. Rusetsky, Nucl. Phys. B 806 (2009) 178.